

Protein Science

Using structural analysis to generate parasite-selective monoclonal antibodies

Michael A. Kron, Sam Cichanowicz, Angela Hendrick, Aizhuo Liu, Joseph Leykam and Leslie A. Kuhn

Protein Sci. 2008 17: 983-989; originally published online Apr 14, 2008;
Access the most recent version at doi:[10.1110/ps.073429808](https://doi.org/10.1110/ps.073429808)

Supplementary data

"Supplemental Research Data"

<http://www.proteinscience.org/cgi/content/full/ps.073429808/DC1>

References

This article cites 31 articles, 4 of which can be accessed free at:

<http://www.proteinscience.org/cgi/content/full/17/6/983#References>

Email alerting service

Receive free email alerts when new articles cite this article - sign up in the box at the top right corner of the article or [click here](#)

Notes

To subscribe to *Protein Science* go to:
<http://www.proteinscience.org/subscriptions/>

Using structural analysis to generate parasite-selective monoclonal antibodies

MICHAEL A. KRON,¹ SAM CICHANOWICZ,² ANGELA HENDRICK,³ AIZHUO LIU,⁴ JOSEPH LEYKAM,⁵ AND LESLIE A. KUHN⁶⁻⁹

¹Department of Medicine, Biotechnology and Bioengineering Center, Medical College of Wisconsin, Milwaukee, Wisconsin 53226, USA

²Biotechnology and Bioengineering Center, Medical College of Wisconsin, Milwaukee, Wisconsin 53226, USA

³College of Human Medicine, Michigan State University, East Lansing, Michigan 48824, USA

⁴Department of Biochemistry and Molecular Biology, Michigan State University, East Lansing, Michigan 48824, USA

⁵Macromolecular Structure, Sequence, and Synthesis Facility, Department of Biochemistry and Molecular Biology, Michigan State University, East Lansing, Michigan 48824, USA

⁶Department of Biochemistry and Molecular Biology, Michigan State University, East Lansing, Michigan 48824, USA

⁷Department of Computer Science and Engineering, Michigan State University, East Lansing, Michigan 48824, USA

⁸Department of Physics and Astronomy, Michigan State University, East Lansing, Michigan 48824, USA

⁹Quantitative Biology Initiative, Michigan State University, East Lansing, Michigan 48824, USA

(RECEIVED January 4, 2008; FINAL REVISION March 12, 2008; ACCEPTED March 13, 2008)

Abstract

Diagnosis of eukaryotic parasitic infection using antibody-based tests such as ELISAs (enzyme-linked immunosorbent assays) is often problematic because of the need to differentiate between homologous host and pathogen proteins and to ensure that antibodies raised against a peptide will also bind to the peptide in the context of its three-dimensional protein structure. Filariasis caused by the nematode, *Brugia malayi*, is an important worldwide tropical disease in which parasites disappear from the bloodstream during daylight hours, thus hampering standard microscopic diagnostic methods. To address this problem, a structural approach was used to develop monoclonal antibodies (mAbs) that detect asparaginyl-tRNA synthetase (AsnRS) secreted from *B. malayi*. *B. malayi* and human AsnRS amino acid sequences were aligned to identify regions that are relatively unconserved, and a 1.9 Å crystallographic structure of *B. malayi* AsnRS was used to identify peptidyl regions that are surface accessible and available for antibody binding. Sequery and SSA (Superpositional Structural Analysis) software was used to analyze which of these peptides was most likely to maintain its native conformation as a synthetic peptide, and its predicted helical structure was confirmed by NMR. A 22-residue peptide was synthesized to produce murine mAbs. Four IgG₁ mAbs were identified that recognized the synthetic peptide and the full-length parasite AsnRS, but not human AsnRS. The specificity and affinity of mAbs was confirmed by Western blot, immunohistochemistry, surface plasmon resonance, and enzyme inhibition assays. These results support the success of structural modeling to choose peptides for raising selective antibodies that bind to the native protein.

Keywords: aminoacyl-tRNA synthetase; filariasis; surface plasmon resonance; nuclear magnetic resonance; conformational determinacy; *Brugia malayi*; epitope prediction

Supplemental material: see www.proteinscience.org

Reprint requests to: Michael A. Kron, Department of Medicine, Biotechnology and Bioengineering Center, Medical College of Wisconsin, 8701 Watertown Plank Road, P.O. Box 26509, Milwaukee, WI 53226, USA; e-mail: mkron@mcw.edu; fax: (414) 456-6568.

Article published online ahead of print. Article and publication date are at <http://www.proteinscience.org/cgi/doi/10.1110/ps.073429808>.

Immunodiagnosis of pathogenic eukaryotic parasites is often problematic because of the need to differentiate between cross-reactive antigens. The World Health Organization ranks 10 human parasitic diseases as priority areas for research that includes the use of genomics to

discover improved therapeutic and diagnostic agents (Nwaka and Hudson 2006). Worldwide, the parasitic disease known as lymphatic filariasis (elephantiasis) affects over 300 million persons in developing countries. Adult filarial parasites are inaccessible deep inside the host lymphatic system, and immature larvae (microfilariae) frequently exhibit a nocturnal periodicity and disappear from the bloodstream during daylight hours (King and Freedman 2000). Diagnosis of filariasis also is hampered by a lack of inexpensive, sensitive, and specific immunoassays that can be used in daytime blood tests.

Recently, it has been shown that the filarial parasite enzyme asparaginyl-tRNA synthetase (AsnRS), an acknowledged target for new antiparasite drug discovery (Kron et al. 2003b; Sukuru et al. 2006), also is an abundant and antigenic protein that is actively excreted/secreted from adult and larval parasites (Kron et al. 2000). Aminoacyl-tRNA synthetases (AARS) are a family of heterogeneous enzymes involved in protein biosynthesis, and they are grouped into two classes in both prokaryotes and eukaryotes based on catalytic site topology and overall protein fold (Cusack et al. 1990; Ibba and Soll 2001). Within a class, each AARS exhibits three highly conserved motifs distributed within a poorly conserved amino-terminal domain and a more highly conserved carboxy-terminal region (Weiner 1999; Ibba et al. 2000). Human cytoplasmic AsnRS is a class II AARS expressed in many human tissues, particularly in the pancreas, skeletal, and cardiac muscle (Kron et al. 2005). A wide range of secondary functions of AARS have been documented in various species, including roles in transcriptional regulation, mitochondrial RNA splicing, control of cell growth, and cytokine- or chemokine-like activity (Martinis et al. 1999).

Several approaches have been developed by other groups for identifying antibody-binding (or "B cell") epitopes on proteins. The simplest case is when the epitope is a linear sequence forming a continuous structure bound by the antibody, e.g., an exposed loop or the edge of a β -strand. Even an epitope that is part of an α -helix (a continuous structure) is generally comprised of residues that are not contiguous in the sequence, because one face of the helix is solvent exposed and available for antibody binding, while the other is buried against the protein. A stripe of helical residues thus forms a conformational rather than linear epitope. Methods for predicting epitopes (Van Regenmortel 1996; Korber et al. 2006; Greenbaum et al. 2007) generally focus on either linear or conformational epitopes, and many use sequence features (predicted secondary structure, hydrophobicity, solvent exposure, protrusion, sequence variability, and flexibility values) (Alix 1999; Bublil et al. 2007; Joshi 2007), while others use information derived from 3D protein structures and their dynamics (Zvelebil et al. 1993; Kulkarni-Kale et al. 2005; Haste Andersen et al. 2006; Gonzalez-Ruiz and Gohlke 2006).

The goal of the Sequery/SSA method described below is to identify sequences in a folded protein that are most likely to form the same structure as a short peptide in solution. This increases the likelihood that a mAb raised against the peptide will be able to recognize, or cross-react with, the corresponding epitope in the folded protein. This issue of structural self-determinacy of short amino acid sequences turns out to be interesting, because some sequences, e.g., YXRF, are highly structurally self-determinate and form the same structure (in this case, a β -turn) (Collawn et al. 1990) in diverse proteins, whereas other sequences are structurally plastic (Wilson et al. 1985), and their conformation depends almost entirely on their three-dimensional structural context (e.g., the four residue sequence pattern G[R,K][R,K]K, which is equally distributed between helical, irregular, and undefined or hyperflexible structures in different proteins). The Sequery/SSA approach to identify the subset of surface-exposed peptides that are structurally self-determinate was validated for myohemerythrin and hen egg-white lysozyme, in which the selected peptides were shown to elicit antibodies that cross-reacted with the intact proteins (Craig et al. 1998).

To address the problem of developing a mAb assay to detect *Brugia* AsnRS without false positives due to cross-reacting with the endogenous human AsnRS, structural analysis of the *Brugia* AsnRS was used to select the *Brugia* AsnRS peptide most likely to produce parasite specific murine mAbs. Combining this approach with selecting epitopes that differ most between the *Brugia* and human proteins, four mAbs were generated that are specific for *Brugia* AsnRS and intensely stain *Brugia* embryos and larvae. Monoclonal antibodies with the highest affinity for parasite AsnRS have been donated to Dr. Bernadette Libranda-Ramirez of the Philippines National Institutes of Biotechnology and Molecular Biology to field test antigen capture assays for daytime diagnosis of filariasis in the Philippines, where 20 million persons live in areas where nocturnally periodic filariasis is actively transmitted (Kron et al. 2000).

Results

Alignment of the *B. malayi* and human AsnRS amino acid sequences using BESTFIT (GCG) correctly aligned the three conserved motifs in class II AARS, while also allowing identification of several regions that were <50% identical in amino acid sequence, including the whole amino-terminal domain (107 residues) and regions flanking the three short highly conserved motifs that are characteristic of class II AARS (Supplemental Fig. 1). A 1.9 Å resolution atomic structure of *B. malayi* AsnRS lacking the amino-terminal domain, which is inessential for catalytic function, was provided by collaborator Stephen Cusack (EMBL Grenoble) (F. Danel, P. Caspers,

S.C.K. Sukuru, L. Kuhn, T. Crepin, S. Cusack, M. Grotli, M. Haertlein, M. Kron, C. Berthet-Colominas, et al., in prep.) Peptides with low sequence identity between *Brugia* and human AsnRS were filtered to identify those that are solvent accessible, based on molecular graphics visual inspection of the *Brugia* structure. Three peptide sequences were selected for further analysis by Sequery and SSA.

These regions in the *B. malayi* AsnRS sequence were analyzed using the computer software Sequery and SSA. Sequery (Collawn et al. 1990; Craig et al. 1998) was used to search for all instances of similar tetrapeptide sequences in a set of 2832 Protein Data Bank chains with crystallographic resolution of 2.0 Å or better, *R* factors of 0.25 or less, and <25% sequence identity with each other (Wang and Dunbrack Jr. 2003) (<http://dunbrack.fccc.edu/PISCES.php>). SSA was used to assign the secondary structure of each match from the Protein Data Bank, based on closeness of superposition of the matched tetrapeptide with a set of α -helix, reverse turn (type 1, 1', 2, 2', etc.), and β -strand templates. (Note: Sequery and SSA software packages are available for downloading from <http://www.bmb.msu.edu/~kuhn>.) The three surface-exposed sequences chosen for analysis based on having significant sequence difference between *Brugia* and human AsnRS were: (1) residues 6–19 (yellow) in the amino-terminal truncated form of AsnRS (RDLVKHRNERVCIK), an exposed region that is partly an irregular helix followed by a loop and a β -strand, (2) residues 55–79 (TYDALTVN

TECTVEIYGAIKEVPEG, purple), a helix and a β -strand linked by a short buried loop, and (3) residues 370–382 (KFDELSKAFKNVE, red), a highly exposed α -helix (Fig. 1). Residue numbers are from the A chain of the crystal structure of *B. malayi* AsnRS bound to Asn-sulfamoyl-adenylate (available upon request from Stephen Cusack, cusack@embl-grenoble.fr). Because the third peptide forms an α -helix stabilized by intrapeptide main-chain hydrogen bonds, it was expected that this region would be more structurally independent of the surrounding protein. According to Sequery and SSA, this peptide also showed the strongest regular secondary structural propensity of the three peptides, based on sequence matches in diverse Protein Data Bank entries (Supplemental Table 1). Fifty percent to 100% of the overlapping tetrapeptide matches in the central 11 of the 13 residues were found to be helical, suggesting that this region could fold in a native-like conformation in solution.

To produce mAbs against *Brugia* AsnRS, this peptide was synthesized with blocked, neutral termini chosen to represent the state of the peptide in the context of the AsnRS structure. Three flanking residues from the native sequence were added at the N terminus, and four were added at the C terminus to compensate for the tendency of peptidyl termini to unravel in solution. The peptide RIWKDFDELSKAFKNVEIDPK was produced on an Applied Biosystems synthesizer and HPLC purified. Mass spectrometry analysis confirmed its molecular mass, showing a strong peak at 1555 *m/z*. Nuclear magnetic

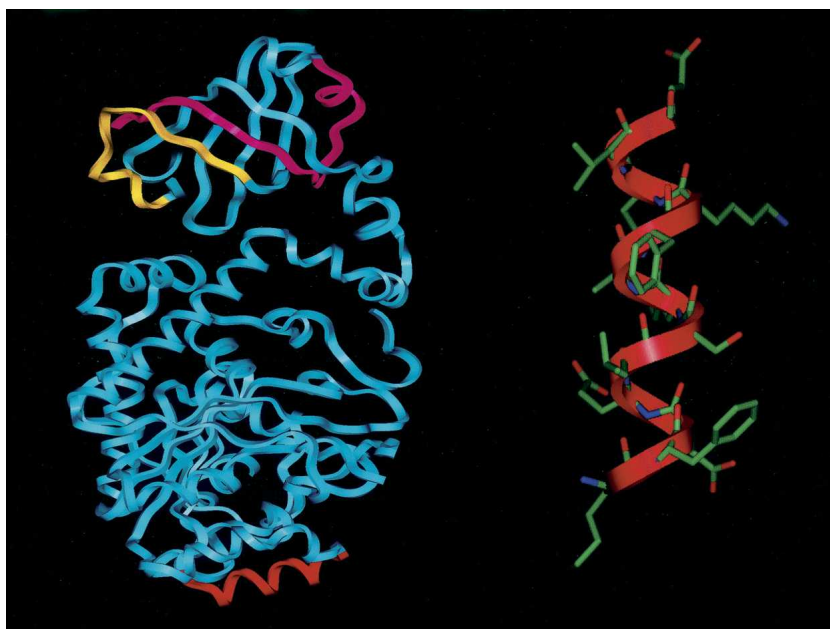


Figure 1. Ribbon diagram of a monomer (*left*) of the *Brugia malayi* asparaginyl-tRNA synthetase dimer. Three surface peptide regions analyzed by Sequery and SSA are shown in yellow, purple, and red, corresponding to peptides 1, 2, and 3. The core region of peptide 3, KFDELSKAFKNVE, chosen for antibody production, is shown on the *right*.

resonance (NMR) spectroscopy was used to confirm the existence of α -helical conformation of the synthetic peptide prior to its use for mAb production (Fig. 2). Proton resonance assignment of the peptide, RIWKFD~~ELSKAF~~KNVEIDPK, was achieved by using conventional homonuclear two-dimensional NMR spectroscopy, through the combined analysis of COSY, TOCSY, and NOESY spectra (Wüthrich 1986). Figure 2A shows the amide proton ($^1\text{H}^{\text{N}}$) region of the NOESY spectrum together with the secondary α -proton ($^1\text{H}^{\alpha}$) chemical shifts. The strong sequential ($^1\text{H}^{\text{N}}$) correlation and the continuous negative secondary ($^1\text{H}^{\alpha}$) chemical shifts in the D6–A11 region of the peptide indicate a significant population of α -helical conformation.

The peptide RIWKFD~~ELSKAF~~KNVEIDPK was used to immunize Balb/C mice for production of mAbs

using three subcutaneous injections with 50 μg of KLH-conjugated peptide. Ultimately, three IgG₁ mAbs were identified by strong reactivity with the original synthetic peptide. Binding kinetics of each IgG₁ mAb to the native 63 kDa *B. malayi* AsnRS were studied by surface plasmon resonance (SPR) (Hahnefeld et al. 2004). Relative dissociation constants (K_d values) were used to rank the affinity of each mAb (Fig. 2B). The SPR data revealed two different patterns of association curves. Although mAb 3B4 demonstrated the fastest binding, mAb 3D6 exhibited the lowest relative K_d of 140 nM (Table 1), and thus was chosen for immunohistochemical studies. All four mAbs were of the IgG₁ isotype and reacted strongly and specifically with full-length (548 amino acids) and amino-terminal truncated (residues 112–548 remaining) *B. malayi* AsnRS, but not with the full-length human

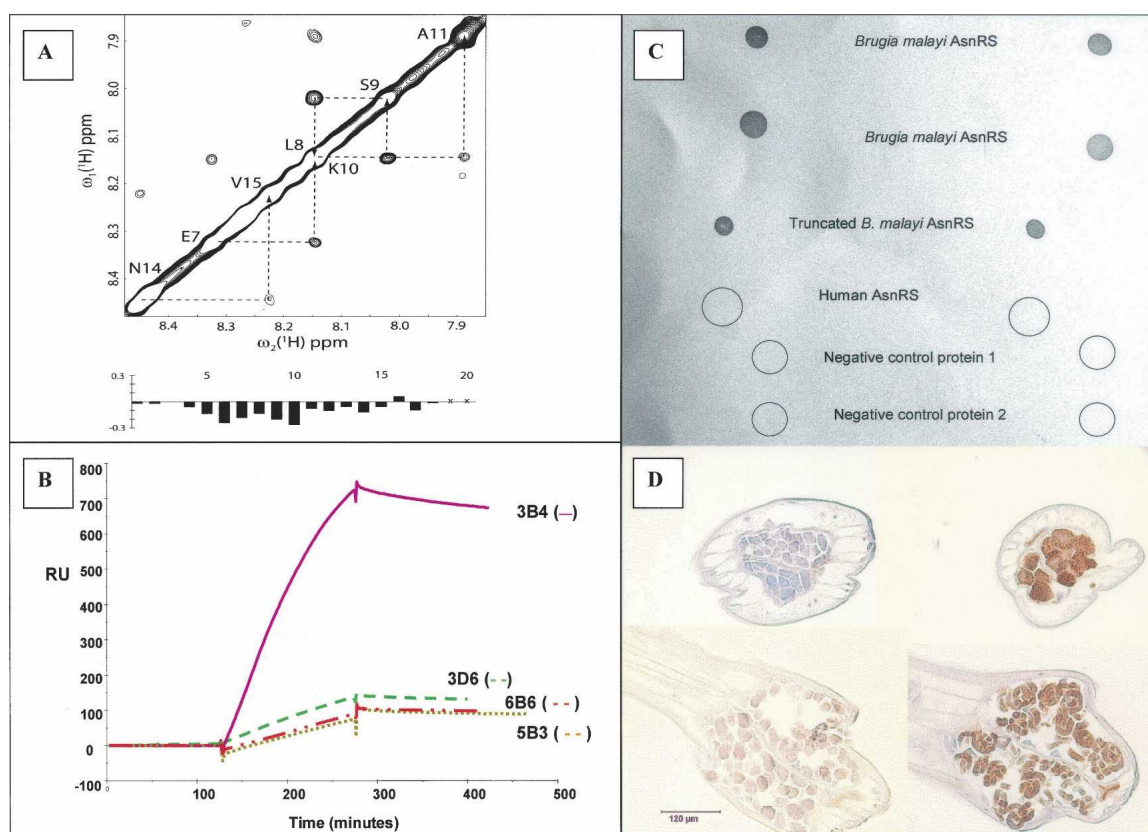


Figure 2. (A) The *upper* panel is the amide region of NOESY spectrum with the peptide RIWKFD~~ELSKAF~~KNVEIDPK. The underlined part indicates the core region targeted for binding, and the flanking residues were added to allow for the likelihood of terminal residues unraveling in solution. The *lower* panel shows the $^1\text{H}^{\alpha}$ secondary chemical shifts (according to residue number within the peptide), which were derived from the α -proton chemical shifts of the peptide after subtracting the corresponding random-coil values. The amide resonance of residue K20 was not observable, and the preceding residue is a proline. The $^1\text{H}^{\alpha}$ chemical shift of D18 was modified due to the neighboring proline effects. (B) Surface plasmon resonance studies of the mAbs binding to full-length *Brugia malayi* identified two patterns of association curves. (C) Immunoblot representative of four IgG₁ mAbs reactive with native *B. malayi* AsnRS and 1–110 amino terminus truncated *B. malayi* AsnRS. Unrelated proteins (control 1: bovine serum albumin, control 2: *E. coli* protein) and recombinant human AsnRS were not immunoreactive. (D) Immunostaining of adult *Brugia malayi* using mAb 3D6. (*Upper left*) Cross-section of female worm-negative IgG₁ isotype control showing distribution of embryos (*center*) and poorly visualized muscle cells under the cuticle. (*Lower left*) Sagittal section of negative control mature female worm. (*Upper right*) Immunostaining (brown) of intrauterine embryos and larvae with mAb 3D6. (*Lower right*) Intense immunostaining of intrauterine structures using mAb 3D6.

Table 1. Kinetic data from mAb binding to *Brugia AsnRS* determined SPR

Monoclonal antibody	K_a (1/ms)	K_d (1/s)	R_{max} (RU)	K_a (1/M)	K_d (M)	χ^2
6B6	7.2E + 01	5.40E - 04	2.40E + 04	1.30E + 05	7.50E - 06	8.40E + 00
5B3	2.60E + 02	5.70E - 04	6.40E + 03	4.60E + 05	2.20E - 06	1.80E + 00
3B4	5.2E + 01	1.40E - 03	2.90E + 05	3.70E + 04	2.70E - 05	2.10E + 02
3D6	8.10E + 03	1.10E - 03	3.00E + 02	7.40E + 06	1.40E - 07	1.20E + 00

AsnRS or unrelated proteins in stringent dot blot analysis (Fig. 2C). Immunohistochemical studies of formalin fixed *B. malayi* parasites using mAb 3D6 revealed strong staining in both adult male and female parasites (Fig. 2D) and in microfilariae (juvenile worms). In addition to showing specificity and affinity for the filarial AsnRS, the mAbs also inhibited enzyme activity. A malachite green pyrophosphatase assay that measures enzyme-generated phosphate was used to measure the inhibitory activity of mAbs (Danel et al. 2004; Newton et al. 2006). Purified mAbs at concentrations of 5 μ g per mL, diluted up to 1:10,000, all exhibited significant neutralization of AsnRS activity (Table 2). Enzyme inhibition can be explained by the proximity of the KFDELSKAFKNVE peptide to the active site of AsnRS (Supplemental Fig. 3). Similarly, monoclonal antibody 3D6 was shown to inhibit AsnRS-induced chemotaxis in HEK293 cells stably transfected with CXCR2 (Supplemental Fig. 4). AsnRS induced chemotaxis of human leukocytes via interleukin-8 receptors (CXCR1 and CXCR2) is believed to play a role in the inflammatory response and/or immunosuppression induced by *Brugia* infection in humans (Ramirez et al. 2006).

Discussion

There are many technological and economic challenges for development of improved immunodiagnostic assays in developing countries. Relative lack of scientific infrastructure and smaller research budgets focused on local research compound the problems inherent in diagnosis of immunologically complex tropical diseases. The so-called “10/90 gap” refers to the fact that 90% of global medical research is targeted at problems affecting only 10% of the world’s population (World Health Organization 2002). In the case of mAb production, while basic protein production and purification methods could be reproduced almost anywhere in the world, for the sake of cost containment there is a need to use production strategies that minimize the number of antibodies generated for subsequent detailed evaluation. The computational methods described here can potentially make the generation of species-selective mAbs more successful and cost-efficient. Prior to these efforts to generate AsnRS specific mAbs, the use of polyclonal rabbit IgG and chicken IgY against *Brugia* AsnRS did not yield antibody with the necessary specificity.

The two distinct sets of association curves obtained by surface plasmon resonance suggest that mAb 3B4 may bind to a different epitope than 3D6, 6B6, or 5B3, and this possibility is a focus of current antibody-mediated inhibition competition studies. The K_d of mAb 3D6 was measured using whole IgG₁ mAb and confirmed using Fab fragments of 3D6, which generated the same K_d value of 140 nM. In addition to generating selective mAbs, these mAbs neutralize two distinct biological activities of AsnRS: aminoacylation and IL-8 receptor-mediated chemotaxis. Thus, these mAbs can be used to investigate the biological sequelae of AsnRS inhibition, apart from their utility for disease diagnosis. The structure-based approach for generating antibodies presented here is expected to facilitate new successes in raising diagnostic antibodies against the AARS of human pathogens and against many other protein antigens.

Materials and Methods

Murine mAb production

Balb/C mice received three injections of KLH-conjugated peptide, KFDELSKAFKNVE, by Washington Biotechnology, Inc., and were assessed for sufficient titer by ELISA 10 days after their third injection. Mice with titers >50,000 were chosen for the myeloma fusion procedure. Myeloma fusions that produced anti-peptide mAb were isolated by limiting dilution and designated 3D6, 3B4, 5B3, and 6B6. MAb were purified using the Millipore Montage Prosep-A spin column kit (Millipore

Table 2. Aminoacylation inhibition assays using monoclonal antibody 3D6

	OD	% Inhibition	Final dilution of inhibitor (μ g/mL)
BmAsnRS without inhibitor	0.99 \pm 0.17	n/a	0
Positive control			
Asn-S-adenylate	0.21 \pm 0.02	100%	7.81 ^a
3D6	0.13 \pm 0.01	100%	4.98
3D6	0.24 \pm 0.01	98%	4.98 \times 10 ⁻¹
3D6	0.18 \pm 0.05	100%	4.98 \times 10 ⁻²
3D6	0.19 \pm 0.01	100%	4.98 \times 10 ⁻³
3D6	0.18 \pm 0.04	100%	4.98 \times 10 ⁻⁴
Control IgG ₁	1.35 \pm 0.06	0%	5.82

^aEquivalent to 17 μ M.

#LSK2AGA20), and the isotype was identified using a mouse mAb isotyping kit (GE Healthcare # RPN29).

Western blot assays

One microgram of test antigens (recombinant *B. malayi* AsnRS wild type, an amino-terminal truncated *B. malayi* AsnRS missing residues 1–111, bovine serum albumin [BSA], and *E. coli* extract proteins) were spotted onto nitrocellulose membranes. After blocking filters with 3% BSA, a 1:1000 dilution of each one of the mAbs was incubated with the membrane for 3 h at 4°C, washed, and incubated with 1:100 dilution of mouse anti-IgG conjugated to HRP. Diaminobenzidine (DAB) substrate was used to localize the secondary antibody-bound mAb complex.

Surface plasmon resonance (SPR)

Affinities between *B. malayi* AsnRS and each of the three IgG1 mAbs were measured by biosensor technology using the BIAcore 3000 (GE Healthcare) and CM5 sensor chips. *B. malayi* AsnRS was amine coupled using 1-ethyl-3-(3-dimethylaminopropyl) carbodiimide (EDC) and N-hydroxysuccinimide (NHS) to bind/immobilize the protein onto the CM5 sensor chip. Sensorgrams were obtained using five concentrations and were fit locally to the 1:1 model of interaction by using the Fit Kinetics:Separate K_a/K_d program in the BIA evaluation software for flow cell 3-1, to allow for analytical integration in each one of the separate association and dissociation phases. Resonance units (RU) are a measure of bound protein in a given experiment, and one RU represents ~ 1 pg of protein per square millimeter of sensor chip surface. The dissociation constant was calculated by using 50 s of data points to calculate a global-fit K_d value. In the association fit, the K_d value from the dissociation fit was used as a global parameter, and K_a and R_{max} were fit globally using 50 s of data points (Johnsson et al. 1991).

The CM5 sensor chip was activated by injection of a 1:1 ratio of NHS/EDC, 50 μ L of 0.05 M N-hydroxysuccinimide and 0.2 M 1-ethyl-3-(3-dimethyl-aminopropyl) carbodiimide followed by injection of 210 μ L of a 1.5 mg/mL solution of *Brugia malayi* AsnRS diluted in 10 mM sodium acetate (pH 4.5), providing a high density surface. The uncoupled/unreacted ester groups on the CM5 chip were blocked by injection of 50 μ L of 1 M ethanolamine-HCl (pH 8.5). All steps were performed at a flow rate of 5 μ L/min. Flow cell one of each chip did not contain *B. malayi* AsnRS, and was used for reference correction. Monoclonal antibodies were diluted in flow buffer and injected at a flow rate of 20 μ L/min for 2.5 min using the K_{inject} program, followed by a dissociation phase of 2 min in running buffer.

Immunohistochemistry

Adult male and female *B. malayi* were obtained from the laboratory of Dr. John McCall (Athens, Georgia) under an NIH supply contract. Parasites were fixed in 0.1% buffered formalin and embedded in paraffin blocks for sectioning. Thin sections were used for both hematoxylin and eosin staining for morphology, as well as immunochemical staining using mAb 3D6. *Brugia* sections were blocked with 3% BSA, then incubated with 1:1000 dilution of 3D6 in phosphate-buffered saline, pH 7.4, and bound primary antibody was localized using anti-mouse IgG conjugated to horseradish peroxidase. DAB substrate, which gives a brown coloration under light microscopy,

was used to identify the distribution of the 3D6-anti-mouse IgG complex.

NMR spectroscopy

All NMR spectra were recorded on a Varian INOVA 600 MHz spectrometer at 20°C. NMR raw data were processed with the NMRPipe (Delaglio et al. 1995) package and analyzed with the NMRView (Johnson 2004) software. The cross-relaxation mixing time of the NOESY experiment was set to 300 ms. The ^1H isotropic mixing time of the TOCSY experiment was set to 75 ms. Peptide powder was directly solved in 90%/10% $\text{H}_2\text{O}/\text{D}_2\text{O}$ solution without any buffer because phosphate buffer was found to decrease the solubility of the peptide. The NMR sample concentration was about 0.5 mM at pH 5.5. A trace amount of 2,2-dimethyl-2-silapentane-5-sulfonate sodium salt (DSS) was added into the solution as the inner ^1H chemical shift reference.

Aminocyclation inhibition assays

Stock solutions of mAb 3D6 were diluted 10-fold to 1:10,000 using HEPES-buffered saline. Enzyme inhibition studies were conducted using a malachite green-based assay that measures the production of phosphate via the release of pyrophosphate as a by-product of AsnRS activity (Danel et al. 2004; Newton et al. 2006). Equal volumes of diluted AsnRS and mAb or control inhibitor were incubated in 96-well microtiter plates at 4°C for 2 h, after which 24 μ L of a mixture containing 6 μ L 0.5 M HEPES, 0.6 μ L 0.2 M magnesium acetate, 7.5 μ L L-cysteine, 3 μ L 0.125 M dithiothreitol, and 1.5 μ L deionized water was added to each well. Thirty microliters of a mixture of 1.5 μ L 10 mM L-aspartate β -hydroxamate, 0.75 μ L 100 U/mL pyrophosphatase (Roche, catalogue #10108987001), 1.5 μ L 0.5 M HEPES, 1.5 μ L 0.2 M Mg acetate, 1.5 μ L 50 mM ATP pH 7.0, and 23.35 μ L water were added to each well and incubated at 37°C for 4 h. Sixty-four microliters of malachite green solution were added to each well and mixed for 10 min at room temperature in the dark. The OD was measured at 620 nm using a PowerWave XS Universal Microplate Spectrophotometer (BioTek, catalogue #MQX200R).

Chemotaxis assays

An HEK293 cell line stably transfected with CXCR2 (a gift from Dr. O.M. Zack-Howard, National Cancer Institute) was resuspended in RPMI 1640 binding media at $1\text{--}5 \times 10^6$ cells/mL, enriched with 1% bovine serum albumin, 25 mM HEPES, pH 8.0. Chemotaxis assays were conducted in 48-well Neuroprobe Boyden chambers using 10 μ M polycarbonate membranes pre-coated with 50 μ g/mL of rat tail collagen type I (BD Bioscience) at 37°C for 2 h. Monoclonal antibody 3D6 and human IgG, normal serum (Bethyl Laboratories, Inc.) were diluted in binding media containing 10 ng/mL BmAsnRS and placed in the lower wells of a chemotaxis chamber. Fifty microliters of HEK293-CXCR2 suspension (cell density) were placed in the upper wells. The filled chemotaxis chambers were incubated in a humidified CO_2 incubator for 5 h. HEK293-CXCR2 transfected cells were also pre-incubated with 10 μ g/mL of anti-CXCR2 antibody (R&D) for 30 min at 37°C. The CXCR2 antibody was used in this study as a positive control for a blocking chemotaxis activity. After the incubation membranes were removed from the chemotaxis chamber assembly, the cells from the upper side of the membrane were gently removed by

rinsing in PBS solution, whereas the cells from the lower side of the membrane were fixed and stained using Rapid Stain (Richard-Allen Scientific). Cells that crossed membrane were counted under a microscope using 200× magnification.

Electronic supplemental material

Supplemental Table 1: sequery and SSA analysis for *Brugia* AsnRS; Supplemental Figure 1: alignment of the amino acid sequences of *Brugia* and human AsnRS; Supplemental Figure 2: NMR data analysis of synthetic peptide RIWKFDELSKAFKN VEIDPK; Supplemental Figure 3: model of how monoclonal antibody neutralizes enzymatic activity of *Brugia* AsnRS; and Supplemental Figure 4: chemotaxis inhibition assays using comparing mAb 3D6 to anti-CXCR2.

Acknowledgments

This work was supported in part by grants from the U.S. National Institutes of Health (NIAID U01 A153877) to M.A.K. and L.A.K., and grants from the Fogarty International Center (RO3 TW01092), and an NIH Minority International Research Training Grant (T37 TW00052) to M.A.K. Adult *Brugia malayi* were generously supplied by John McCall from the N.I.H. Filaria Repository (contract NO-165283). Stephen Cusack, from the European Molecular Biology Laboratory, provided three-dimensional crystallographic coordinates for the 1.9 Å resolution structure of *B. malayi* AsnRS. Snjezana Kutlesa provided technical assistance with HEK293 chemotaxis assays, and Jessica Kopaczewski provided technical assistance with enzyme inhibition assays using monoclonal antibodies. Lynn Gruman from the Children's Research Institute Histology and Imaging Core at the Medical College of Wisconsin provided technical expertise with immunohistochemical staining.

References

- Alix, A.J. 1999. Predictive estimation of protein linear epitopes by using the program PEOPLE. *Vaccine* **18**: 311–314.
- Bublil, E.M., Freund, N.T., Mayrose, I., Penn, O., Roitburd-Berman, A., Rubinstein, N.D., Pupko, T., and Gershoni, J.M. 2007. Stepwise prediction of conformational discontinuous B-cell epitopes using the Mapitope algorithm. *Proteins* **68**: 294–304.
- Collawn, J.F., Stangel, M., Kuhn, L.A., Esekogwu, V., Jing, S.Q., Trowbridge, I.S., and Tainer, J.A. 1990. Transferrin receptor internalization sequence YXRF implicates a tight turn as the structural recognition motif for endocytosis. *Cell* **63**: 1061–1072.
- Craig, L., Sanschagrin, P.C., Rozek, A., Lackie, S., Kuhn, L.A., and Scott, J.K. 1998. The role of structure in antibody cross-reactivity between peptides and folded proteins. *J. Mol. Biol.* **281**: 183–201.
- Cusack, S., Berthet-Colominas, C., Haertlein, M., Nassar, N., and Leberman, R. 1990. A second class of synthetase structure revealed by X-ray analysis of *E. coli* seryl-tRNA synthetase at 2.5 Å. *Nature* **349**: 249–255.
- Danel, F., Walle, C., Kron, M., Haertlein, M., Cusack, S., and Page, M. 2004. Pre-transfer editing in *Brugia malayi* asparaginyl tRNA synthetase. In *International workshop on aminoacyl tRNA synthetases*, p. 115. Seoul National University, Seoul, Korea.
- Delaglio, F., Grzesiek, S., Vuister, G.W., Zhu, G., Pfeifer, J., and Bax, A. 1995. NMRPipe: A multidimensional spectral processing system based on UNIX pipes. *J. Biomol. NMR* **6**: 277–293.
- Gonzalez-Ruiz, D. and Gohlke, H. 2006. Targeting protein–protein interactions with small molecules: Challenges and perspectives for computational binding epitope detection and ligand finding. *Curr. Med. Chem.* **13**: 2607–2625.
- Greenbaum, J.A., Andersen, P.H., Blythe, M., Bui, H.H., Cachau, R.E., Crowe, J., Davies, A.S., Kolaskar, O., Lund, S., Morrison, B., et al. 2007. Towards a consensus on data sets and evaluation metrics for developing B-cell epitope prediction tools. *J. Mol. Recognit.* **20**: 75–82.
- Hahnfeld, C., Drewianka, S., and Herberg, F.W. 2004. Determination of kinetic data using surface plasmon resonance biosensors. *Methods Mol. Med.* **94**: 299–320.
- Haste Andersen, P., Nielsen, M., and Lund, O. 2006. Prediction of residues in discontinuous B-cell epitopes using protein 3D structures. *Protein Sci.* **15**: 2558–2567.
- Ibba, M. and Soll, D. 2001. The renaissance of aminoacyl-tRNA synthetases. *EMBO J.* **2**: 382–387.
- Ibba, M., Becker, H.D., Saphopoulos, C., Tumbula, D.L., and Soll, D. 2000. The Adaptor Hypothesis revisited. *Trends Biochem. Sci.* **25**: 311–316.
- Johnson, B.A. 2004. Using NMRView to visualize and analyze the NMR spectra of macromolecules. *Methods Mol. Biol.* **278**: 313–352.
- Johnsson, B., Lofas, S., and Lindquist, G. 1991. Immobilization of protein to a carboxymethyl dextran modified gold surface for biospecific interaction analysis in surface plasmon resonance sensors. *Anal. Biochem.* **198**: 269–277.
- Joshi, R.R. 2007. Peptide vaccine models using statistical data mining. *Protein Pept. Lett.* **14**: 536–542.
- King, C. and Freedman, D. 2000. Filarial infection. In *Hunter's tropical medicine* (ed. G. Strickland), pp. 740–774. Saunders, Philadelphia, PA.
- Korber, B., LaButte, M., and Yusim, K. 2006. Immunoinformatics comes of age. *PLoS Comput. Biol.* **2**: E71. doi: 10.1371/journal.pcbi.0020071.
- Kron, M., Walker, E., Hernandez, L., Torres, E., and Libranda-Ramirez, B. 2000. Lymphatic filariasis in the Philippines. *Parasitol. Today* **16**: 329–333.
- Kron, M., Petridis, M., Milev, Y., Leykam, J., and Hartlein, M. 2003a. Expression, localization and alternative function of cytoplasmic asparaginyl-tRNA synthetase in *Brugia malayi*. *Mol. Biochem. Parasitol.* **129**: 33–39.
- Kron, M.A., Kuhn, L.A., Sanschagrin, P.C., Hartlein, M., Grotli, M., and Cusack, S. 2003b. Strategies for antifilarial drug development. *J. Parasitol.* **89**: S226–S235.
- Kron, M.A., Petridis, M., Haertlein, M., Libranda-Ramirez, B., and Scaffidi, L.E. 2005. Do tissue levels of autoantigenic aminoacyl-tRNA synthetase predict clinical disease? *Med. Hypotheses* **65**: 1124–1127.
- Kulkarni-Kale, U., Bhosle, S., and Kolaskar, A.S. 2005. CEP: A conformational epitope prediction server. *Nucleic Acids Res.* **33**: W168–W171. doi: 10.1093/nar/gki460.
- Martinis, S., Plateau, P., Cavarelli, J., and Florentz, C. 1999. Aminoacyl-tRNA synthetases—a family of expanding functions. *EMBO J.* **18**: 4591–4606.
- Newton, G.L., Ta, P., Sareen, D., and Fahey, R.C. 2006. A coupled spectrophotometric assay for L-cysteine: 1-D-*myo*-inosityl 2-amino-2-deoxy- α -D-glucopyranoside ligase and its application for inhibitor screening. *Anal. Biochem.* **353**: 167–173.
- Nwaka, S. and Hudson, A. 2006. Innovative lead discovery strategies for tropical diseases. *Nat. Rev. Drug Discov.* **5**: 941–955.
- Ramirez, B.L., Zack Howard, O.M., Dong, F.H., Edamatsu, T., Gao, P., Haertlein, M., and Kron, M. 2006. *Brugia malayi* asparaginyl-transfer RNA synthetase induces chemotaxis of human leukocytes and activates G-protein-coupled receptors CXCR1 and CXCR2. *J. Infect. Dis.* **103**: 1164–1171.
- Sukuru, C., Milev, Y., Marsh, L.C., Hill, J.B., Andersen, R.J., Morris, J.C., Rohatgai, A., O'Mahony, G., Grotli, M., Danel, F., et al. 2006. Discovering new classes of *Brugia malayi* asparaginyl-tRNA synthetase inhibitors and relating specificity to conformational changes. *J. Comput. Aided Mol. Des.* **20**: 159–178.
- Van Regenmortel, M.H.V. 1996. Mapping epitope structure and activity: From one-dimensional prediction to four-dimensional description of antigenic specificity. *Methods* **9**: 465–472.
- Wang, G. and Dunbrack Jr., R.L. 2003. PISCES: A protein sequence culling server. *Bioinformatics* **19**: 1589–1591.
- Weiner, A. 1999. Molecular evolution: Aminoacyl-tRNA synthetases on the loose. *Curr. Biol.* **9**: R842–R844. doi: 10.1016/S0960-9822(00)80041-X.
- Wilson, I.A., Haft, D.H., Getzoff, E.D., Tainer, J.A., Lerner, R.A., and Brenner, S. 1985. Identical short peptide sequences in unrelated proteins can have different conformations: A testing ground for theories of immune recognition. *Proc. Natl. Acad. Sci.* **82**: 5255–5259.
- World Health Organization. 2002. Genomics and world health. In *Report to the advisory committee on health research*. World Health Organization, Geneva, Switzerland.
- Wüthrich, K. 1986. *NMR of proteins and nucleic acids*. John Wiley & Sons, Inc., New York.
- Zvelebil, M.J., Tang, L., Cookson, E., Selkirk, M.E., and Thornton, J.M. 1993. Molecular modeling and epitope prediction of gp29 from lymphatic filariae. *Mol. Biochem. Parasitol.* **58**: 145–153.